Saudi Pharmaceutical Journal 32 (2024) 102107

HOSTED BY

Contents lists available at ScienceDirect

Saudi Pharmaceutical Journal

journal homepage: www.sciencedirect.com

Original article

Skin anti-aging potential of *Launaea procumbens* extract: Antioxidant and enzyme inhibition activities supported by ADMET and molecular docking studies

Hanan Khojah [a], Shaima R. Ahmed [a,*], Shahad Y. Alharbi [a], Kholood K. AlSabeelah [a], Hatham Y. Alrayyes [a], Kadi B. Almusayyab [a], Shahad R. Alrawiliy [a], Raghad M. Alshammari [a], Sumera Qasim [b]

[a] Department of Pharmacognosy, College of Pharmacy, Jouf University, Sakaka 72341, Saudi Arabia
[b] Department of Pharmacology, College of Pharmacy, Jouf University, Sakaka 72341, Saudi Arabia

ARTICLE INFO

Keywords:
Launaea procumbens
Anti-aging
ADMET
Docking

ABSTRACT

Aging is a natural process that occurs in all living organisms. Particularly, the skin embodies aging since it serves as a barrier between the body and its surroundings. Previously, we reported the wound healing effect of *Launaea procumbens* and identified compounds therein. The study aims to explore the skin anti-aging properties of the plant extract. To that effect, the antioxidant potential of *L. procumbens* methanolic extract (LPM) was assessed using two complementary DPPH and FRAP assays. The enzyme inhibitory effect of the extract on collagenase, elastase, hyaluronidase, and tyrosinase was evaluated to assess the direct skin anti-aging effects. Similarly, the anti-inflammatory activity was evaluated to explore the indirect anti-aging effects via the assessment of extract inhibitory effects on cyclooxygenase-2 (COX-2) and 5-lipoxygenase (5-LOX). In addition, ADMET and molecular docking studies were performed to explore the interaction mechanisms of identified compounds in LPM with target enzymes. LPM demonstrated significant antioxidant activity in DPPH (IC_{50} = 29.08 µg/mL) and FRAP (1214.67 µM FeSO4/g extract) assays. Plant extract showed significant inhibition of collagenase, elastase, hyaluronidase, and tyrosinase (IC_{50} = 52.68, 43.76, 31.031, and 37.13 µg/mL, respectively). The extract demonstrated significant COX-2 and 5-LOX inhibition capacity with IC_{50} values of 8.635 and 10.851 µg/mL, respectively. The molecular docking study revealed the high potential of the identified compounds to bind to the active sites of enzymes crucially involved in the skin aging process. ADMET analysis of the compounds revealed their good absorption, distribution, and metabolism profiles, and they were found to be safe as well. Study findings suggest *L. procumbens* as a promising source for the development of natural skin anti-aging and antioxidant compounds. This, in turn, may facilitate its incorporation into cosmetic formulations after further investigation.

1. Introduction

The aging process is an unavoidable and natural process that impacts multiple body parts, with the skin being one of the most visible parts that experiences significant alterations over time (Ndlovu et al., 2013). The perception and impact of skin aging can vary among individuals and across different cultures. The societal emphasis on youthful appearance can contribute to psychological impacts, affecting self-esteem and well-being worldwide (Gupta and Gilchrest, 2005). Skin is the largest organ of the human body and performs several vital functions. It acts as a protective barrier, regulates body temperature, and plays a role in sensory perception. Skin aging is a natural and complex process influenced by both intrinsic (chronologic) and extrinsic (photoaging) factors. Intrinsic factors are a natural decline in biological functions over time and include genetics, hormonal changes, and metabolism. Extrinsic factors include UV radiation, environmental pollution, smoking, poor nutrition, and a lack of skincare (Fikry et al., 2023, Elgamal et al., 2021). Understanding the factors influencing skin aging and adopting preventive measures can help minimize visible effects and promote healthier skin as individuals aged. Skin aging has an intricate impact on the

* Corresponding author at: College of Pharmacy, Jouf University, Sakaka 72341, Saudi Arabia.
E-mail address: Srmorsi@ju.edu.sa (S.R. Ahmed).

https://doi.org/10.1016/j.jsps.2024.102107

Available online 25 May 2024

structure, function, and appearance of the skin. Among the signs of skin aging are fine lines and wrinkles, loss of skin elasticity, sagging of the skin, irregular pigmentation, and dryness from reduced moisture retention (Younis et al., 2022).

Skin is composed of three layers: the epidermis, dermis, and subcutaneous tissue. The dermal layer is rich in connective tissue and contains various structural proteins, such as collagen and elastin, along with other molecules that form the extracellular matrix (ECM) (Ndlovu et al., 2013, Lawton, 2019, Gilaberte et al., 2016). Collagen and elastin are proteins responsible for the skin's firmness and elasticity. Naturally, they decrease with age, leading to the formation of wrinkles and sagging of the skin. Hyaluronic acid, which contributes to skin hydration and plumpness, diminishes with age, resulting in drier and less supple skin. Tyrosine is a precursor for the synthesis of melanin, the pigment responsible for the color of the skin, hair, and eyes (Cruz et al., 2023).

One of the major contributors to skin aging is UV radiation. Exposure to UV radiation triggers the release of reactive oxygen species (ROS), which causes oxidative stress, the breakdown of collagen and elastin in the ECM, and inflammation. Additionally, the degradation of the ECM is associated with skin aging and is linked to the increased activity of certain enzymes such as collagenase, elastase, and hyaluronidase. While tyrosinase is not directly implicated in the structural aging of the skin, changes in pigmentation (such as age spots or hyperpigmentation) can be associated with the aging process and cumulative sun exposure (Elgamal et al., 2021, Fikry et al., 2023). So inhibiting these enzymes is a useful strategy for fighting against aging and delaying aging signs (Cruz et al., 2023).

Adopting a healthy lifestyle and protecting skin from external factors can significantly slow down the visible signs of the aging process and maintain skin health. Protecting the skin from harmful UV radiation and oxidative stress is an effective strategy in fighting pigmentation, and prematurely aging skin, wrinkles and fine lines. Compounds that help to neutralize the free radicals give skin the boost it needs to look younger and fresher (Huang et al., 2013).

To address skin anti-aging, research focuses on reducing oxidative stress and ECM degradation. The most commonly used anti-aging *in vitro* models are those that assess antioxidant, anti-collagenase, anti-elastase, anti-hyaluronidase, anti-tyrosinase which directly assess the aging effect on certain skin parameters (Cruz et al., 2023). Skin aging is closely related to inflammation, which is characterized by elevated levels of pro-inflammatory mediators. Lipoxygenase (LOX) enzymes induce the release of pro-inflammatory mediators like leukotrienes. Increased LOX activity can result in the excessive production of such mediators. Pro-inflammatory mediators accelerate the aging process, causing the appearance of wrinkles, decreased tissue repair, and loss of elasticity. Cyclooxygenase (COX) enzymes convert archidonic acid into prostaglandins. Overproduction of COX enzymes can result in excessive prostaglandin synthesis, producing persistent tissue inflammation and hastening the aging process. Also, excessive prostaglandins can contribute to the breakdown of collagen and elastin, resulting in wrinkles and loss of skin elasticity (Younis et al., 2023, Guimarães et al., 2021, Fuller, 2019). So the assessment of anti-inflammatory activity could be implemented to determine the indirect effects of aging on skin. Molecular docking, ADME prediction, and other in silico molecular modeling approaches have been applied recently to predict and computationally discover possible drugs for treating a wide range of disorders (Wei et al., 2022).

The use of botanicals and their constituents as cosmeceuticals has gained popularity in recent years. This has led to the development of the aging-related cosmeceuticals market, which is currently one of the largest consumer markets (Younis et al., 2022). The choice of the plant was of great importance due to the intricate nature of the aging process, which encompasses a multitude of factors. The choice of the plant was based on two criteria: its wound repair potential and its antioxidant efficacy, as demonstrated in prior investigations (Ahmed et al., 2022, Khan et al., 2012).

Launaea procumbens is an Asteraceae plant that has traditionally been used for a variety of therapeutic purposes. It has traditionally been used to treat dermatological problems, tumors, and diarrhea (Rawat et al., 2016). The plant's ayurvedic and herbal remedies are used to treat wounds (Wazir et al., 2007), difficult urine discharge, and fertility problems (Wazir et al., 2007). The plant has also been shown to exhibit cytotoxicity attributes (Rawat et al., 2016), antibacterial effects (Parekh and Chanda, 2006), anti-urolithiatic activity (Makasana et al., 2014), protecting kidneys and lungs from CCl_4-triggered damage (Khan et al., 2010, Khan et al., 2012). Flavonoids, phenols, tannins, alkaloids, and coumarins were found in phytochemical screening (Reddy and Mishra, 2012). *Launaea procumbens*' therapeutic properties make it a potential skin anti-aging candidate. More research is needed, however, to explore the prospect of plant extract for skin aging.

Previously, we studied the phytochemical profile of *L. procumbens* aerial parts (Ahmed et al., 2022), which revealed the presence of 16 secondary metabolites of different chemical classes and proved the noteworthy wound healing potential of the plant. The present contribution concerns the skin anti-aging properties of *L. procumbens* extract. Here we conducted an *in vitro* antioxidant and enzyme inhibitory potential of the extract against crucial enzymes for skin remodeling (elastase, hyaluronidase, collagenase, and tyrosinase) alongside the rate-limiting enzymes that control the inflammatory cascade (cyclooxygenase-2 (COX-2) and 5-lipoxygenase (5-LOX)). Additionally, molecular docking and absorption, distribution, elimination, metabolism, and toxicity (ADEMT) studies were performed to evaluate the potential of previously identified compounds to interfere with the aforementioned enzymes.

2. Materials and methods

2.1. Chemicals and materials

DPPH (2,2-Diphenyl-1-picrylhydrazyl), acetate buffer, 2,4,6-tripyridyl-s-triazine (TPTZ), ferric chloride, collagenase (C8051), buffer tricine, N-[3-(2-furyl) acryloyl]-Leu-Gly-Pro-Ala substrate (FALGPA, F5135), porcine pancreatic elastase, succinyl-Ala-Ala-Alap-nitroanilide, Tris-HCl buffer, hyaluronidase enzyme, calcium chloride, sodium hyaluronate, sodium hydroxide, sodium borate, *p*-dimethylaminobenzaldehyde (PDMAB), mushroom tyrosinase, phosphate buffer, L-DOPA, 5-lipoxygenase enzyme, linoleic acid were obtained from Sigma Chemical Co. (St. Louis, MO, USA). COX Colorimetric Inhibitor Screening Assay Kit (No. 701050, Cayman Chemical, Ann Arbor, Michigan, USA). Positive controls, including butylated hydroxytoluene (BHT), epigallocatechin (EGCG), tannic acid, kojic acid, indomethacin, and nordihydroguaiaretic acid (NDGA), were obtained from Sigma Chemical Co. (St. Louis, MO, USA). Methanol and absolute ethanol (99 %) were purchased from Merck (Darmstadt, Germany). All reagents used were of analytical grade.

2.2. Plant material and extraction

In this study, the plant material (aerial parts of *Launaea procumbens*) and the extraction method were utilized as described in (Ahmed et al., 2022). The authentication of the plant material was conducted by Mr. Hamedan Al-Ogereef of the Camel and Range Research Center, Jouf, KSA, and a voucher specimen (Mor-3–2020) was deposited at Pharmacognosy Department, Faculty of Pharmacy, Deraya University, Egypt. The extraction process involved the use of methanol, and the resulting methanolic extract (LPM) was processed in accordance with the procedures detailed in (Ahmed et al., 2022).

2.3. In vitro antioxidant activity

2.3.1. Radical scavenging activity (DPPH) assay

The procedure outlined by (Ghareeb et al., 2018) was employed to

assess the tested extract's free radical scavenging activity (DPPH). Absolute ethanol (99 %) was used to prepare a 0.06 mM DPPH solution. A total of 200 µL was obtained by equally mixing samples in a concentration range of 6.25–400 µg/mL with DPPH solution (100 µL of DPPH reagent was mixed with 100 µl of sample). Using a microplate spectrophotometer (TECAN, Inc., Durham, NC, USA), the absorbance was determined at 517 nm following a 30-minute dark incubation period. Every measurement was adjusted using a sample devoid of DPPH solution as the background. The standard used for comparison was butylated hydroxytoluene (BHT). The DPPH radical scavenging capacity was computed with the following formula:

$$\%Inhibition = \frac{Absorbancecontrol - Absorbancesample}{Absorbancecontrol} x100 \quad (1)$$

2.3.2. Ferric reducing antioxidant power (FRAP) assay

(Ghareeb et al., 2018) method was used to determine the tested extract's reducing power activity, with some minor modifications. In summary, a mixture of 10:1:1 was prepared using acetate buffer (300 mM, pH 3.6), 2,4,6-tripyridyl-s-triazine (TPTZ) (10 mM in 40 mM HCl), and $FeCl_3{\cdot}6H_2O$ (20 mM). The combination underwent a 10-minute incubation period at 37 °C. A mixture of 3 mL of FRAP solution and 200 µL of plant extract (50–250 µg/mL) was prepared. After 30 min at 37 °C, the mixture was allowed to react. The absorbance of the colored product, Ferrous-TPTZ, was measured at 593 nm. The reference value was ascorbic acid. The FRAP activity was determined from the linear standard calibration curve prepared with ferrous sulfate. The FRAP value of the extract was represented as µM $FeSO_4$ /g extract.

2.4. Enzyme inhibition activity

2.4.1. Collagenase enzyme inhibitory assay

The collagenase inhibitory test was performed using the protocol developed by (Elgamal et al., 2021) with minor modifications. LPM extract (30 µL) in a concentration range of 15.63–1000 µg/mL was mixed with 10 µL of collagenase from *Clostridium histolyticum* enzyme (0.1 mg/mL), and 60 µL of buffer tricine (50 mM tricine, 10 mM calcium chloride, 400 mM sodium chloride, pH 7.5) and incubated for 20 min. at 37 °C. The blank solution consists of 10 µL enzyme, 80 µL phosphate buffer, and 30 µL samples. Subsequently, the mixture solution, excluding the blank solution, was mixed with 20 µL of N-[3-(2-furyl) acryloyl]-Leu-Gly-Pro-Ala substrate (1 mM FALGPA). After that, the absorbance of the solution was determined after 15 min at 335 nm using a microplate reader (TECAN, Inc., Durham, NC, USA). EGCG was used as a positive control, while the negative control solution consisted of enzyme (10 µL) and phosphate buffer (90 µL). The % inhibition was calculated according to formula (1).

2.4.2. Elastase enzyme inhibitory assay

The elastase inhibitory assay was carried out using the method previously described by (Elgamal et al., 2021), with some modifications. Briefly, porcine pancreatic elastase (10 µL) was mixed with 25 µL of LPM extract in a concentration range of 15.63–1000 µg/mL and Tris-HCl (100 mM, pH 8.0) and incubated at 37 °C for 5 min. Following the incubation time, 20 µL of substrate solution (4.4 mM succinyl-Ala-Ala-Alap-nitroanilide in Tris-HCl buffer) was added to the mixture to initiate the reaction. The absorbance was measured at 410 nm. EGCG was used as a positive control; a negative control was performed using distilled water. The % inhibition was calculated according to formula (1).

2.4.3. Hyaluronidase enzyme inhibitory assay

The hyaluronidase inhibitory impact was assessed using the method reported by (Sklirou et al., 2021), with a few modifications. Plant extract in concentration range of 25–250 µg/mL (50 µL, dissolved in 10 % DMSO) was incubated at 37 °C with hyaluronidase enzyme (10 µL) for 10 min., then calcium chloride (20 µL, 12.5 mM) was added to the mixture and incubated again at 37 °C for 10 min. The reaction mixture was treated with sodium hyaluronate (50 µL) and incubated at 37 °C for 40 min before being treated with sodium hydroxide (0.9 M, 10 µL) and sodium borate (0.2 M, 20 µL) and incubated at 100 °C for 3 min. The reaction mixture was treated with *p*-dimethylaminobenzaldehyde (PDMAB, 67 mM, 50 µL) and incubated at 37 °C for 10 min., and absorbance was measured at 585 nm. Tannic acid was used as the reference standard; a negative control was performed using distilled water. The inhibition of hyaluronidase was expressed as % inhibition according to formula (1).

2.4.4. Tyrosinase enzyme inhibitory assay

The tyrosinase inhibitory experiment was carried out using the method published previously by (Fikry et al., 2023). Plant extract (20 µL) in concentration range of 25–250 µg/mL was mixed with the aqueous solution of mushroom tyrosinase (10 µL, 50 units/mL) and phosphate buffer (pH 6.8, 80 µL) and incubated for 5 min at 37 °C. L-DOPA (90 µL, 2 mg/mL) was then added, and the mixture was incubated for 20 min at 37 °C. The amount of dopa chrome produced was determined at 475 nm. The blank was a phosphate buffer, while Kojic acid was used as a positive control. The tyrosinase inhibition (%) was calculated according to formula (1).

2.5. Anti-inflammatory activity

2.5.1. Cycloxygenase-2 (COX-2) inhibition assay

Cycloxygenase-2 (COX-2) activity was evaluated using COX Colorimetric Inhibitor Screening Assay Kit (701050). The assay was performed in accordance with the manufacturer's protocol. The LPM extract was used in a concentration range of 5–25 µg/mL and the enzyme activity was measured colorimetrically by monitoring the appearance of oxidized N,N,N',N'-tetramethyl-p-phenylenediamine (TMPD) at 590 nm. Indomethacin was used as a positive control.

2.5.2. Lipoxygenase-5 (LOX-5)inhibition assay

The 5-lipoxygenase assay was conducted according to the method described by (Zeraik et al., 2021), with some modifications. LPM extract (10 µL) in a concentration range of 5–25 µg/mL was mixed with sodium phosphate buffer (160 µL, 100 mM, pH 8.0) and 20 µl of 5-lipoxygenase enzyme (human recombinant) and incubated at 25 °C for 10 min. After agitating the mixture, 10 µL of linoleic acid was added and incubated for 10 min at 25 °C. The absorbance was measured at 234 nm, and the % inhibition was calculated using formula (1). Nordihydroguaiaretic acid (NDGA) was used as a reference compound; sample with buffer was used as blank control.

2.6. Statistical analysis

All of the conducted assays were implemented as three distinct and independent experiments. The results were presented as mean value with its corresponding standard deviation (SD). Microsoft EXCEL 2010 program and GraphPad prism software version 8 (San Deigo, CA) were employed for data analysis. Graphic plots of dose–response curves were performed to determine the 50 % inhibitory concentration (IC_{50}).

2.7. Molecular docking and ADMET studies

The MOE software, provided by Chemical Computing Group Inc, was utilized for the molecular docking strategy. The docking experiments were conducted on a Pentium 1.6 GHz workstation with 512 MB memory, running the Windows Operating System. Collagenase (1CGL), elastase (1BRU), hyaluronidase (2PE4), tyrosinase (2YPX), cyclooxygenase-2 (5KIR), and lipoxygenase-5 (IJNQ) crystal structures were obtained from the protein data bank. The modified crystal structure was then imported into MOE software after removing water

molecules, and each hydrogen atom was incorporated into the structure according to its standard geometry. Subsequently, energy reduction was performed using MOPAC 7.0. The generated model underwent a systematic conformation scan using the Site Finder tool in MOE, with default parameters and an RMS gradient of 0.01 kcal/mol. The enzyme was examined in order to analyze its active site, and artificial atoms were created based on the alpha spheres that were produced as a result. The backbone and residues remained constant, and an energy reduction process was conducted. Root mean square deviation values (RMSD) were employed to compare the ligand with its related crystal structure. Docked poses having RMSD values below 1.3 °A were grouped. The pose with the lowest energy after reduction was selected for the next investigation. All compounds were subjected to the same method for docking. Ten distinct conformations were chosen for each compound. Other parameters were kept at their default values. The optimal conformation of each ligand-enzyme complex was determined according to energy factor. The resulting model of the ligand-enzyme complex was then used to calculate energy parameters using the MMFF94x force field energy calculation method and to predict the interactions between the docked compound and the enzyme at the active site. The Absorption, Distribution, Metabolism, Elimination, and Toxicity (ADMET) properties of all identified compounds were assessed using the pkCSM online tool (https://biosig.lab.uq.edu.au/pkcsm/).

3. Results

3.1. In vitro antioxidant

In the DPPH radical scavenging assay, LPM exhibited significant antioxidant capacity in a concentration-dependent manner. The LPM extract displayed a conspicuous antioxidant capacity. The concentration at which LPM was able to scavenge half of the DPPH radical (IC_{50}) was 29.082 ± 1.749 g/mL, compared to BHT (20.72 ± 0.138 g/mL) as a reference. For the FRAP assay, LPM also demonstrated promising reducing power capacity (Table 1) with a value of 1214.67 ± 1.527 μM $FeSO_4$/g extract compared to the positive control, ascorbic acid (4794.7 ± 5.507 μM $FeSO_4$/g extract).

3.2. Enzyme inhibition activity

LPM extract was evaluated for its *in vitro* inhibiting activity against four enzymes involved in skin remodeling and aging, namely, collagenase, elastase, hyaluronidase, and tyrosinase. As outlined in Fig. 1, LPM extract showed the strongest inhibition approaching that of reference inhibitor tannic acid against hyaluronidase at concentration range of 25–250 μg/mL (IC_{50} 31.031 ± 0.455 μg/mL vs. 30.652 ± 0.626 μg/mL), followed by elastase at concentration range of 15.63–1000 μg/mL (IC_{50} 43.767 ± 0.831 μg/mL vs. 33.334 ± 0.299 μg/mL for EGCG), collagenase at concentration range of 15.63–1000 μg/mL (IC_{50} 52.688 ± 0.742 μg/mL vs. 33.662 ± 0.302 μg/mL for EGCG), and showed the least inhibition against tyrosinase at concentration range of 25–250 μg/mL (IC_{50} 37.788 ± 2.642 μg/mL vs. 19.066 ± 0.608 μg/mL for kojic acid).

Table 1
In vitro antioxidant activities of *Launaea procumbens* methanolic extract (LPM).

	DPPH (IC_{50}, μg/mL)	FRAP (μM $FeSO_4$/g extract)
LPM	29.082 ± 1.749	1214.67 ± 1.527
BHT (positive control)	20.721 ± 0.138	–
Ascorbic acid	–	4794.7 ± 5.507

BHT: butylated hydroxytoluene, All values expressed are means ± S.D. of three parallel measurements.

3.3. Anti-inflammatory activity

As illustrated in Fig. 2, LPM extract exhibited a promising and comparable inhibitory activity to that of indomethacin at a concentration range 5–25 μg/mL, with an IC_{50} of 8.635 ± 0.0136 μg/mL vs. 5.696 ± 0.079 μg/mL on COX-2. Furthermore, LPM exhibited a significant 5-LOX inhibitory effect at a concentration range 5–25 μg/mL, with an IC_{50} of 10.851 ± 0.733 compared with the positive control, NDGA, with an IC_{50} of 5.255 ± 0.051 μg/mL.

3.4. Molecular docking and ADMET

A molecular docking approach was employed to predict possible interactions between previously identified compounds (Ahmed et al., 2022) of LPM and target enzymes. The previously identified compounds are listed in Table 2. Molecular docking was conducted to simulate the potential binding configuration of identified compounds towards collagenase, tyrosinase, elastase, and hyaluronidase. All compounds have the capability to establish strong interactions with specifically chosen target proteins. The affinity for binding was obtained and subsequently compared with one another, as illustrated in Table 3. On the basis of binding score ranking, with collagenase, Touruosamine (3) displayed a maximum score of −13.953 kcal/mol; with elastase, a maximum score of −16.814 kcal/mol was displayed by Luteolin 8-C-glucoside (13); the maximum score in the case of hyaluronidase was displayed by isobetanidin (9) with a score of −15.154 kcal/mol; and Cimigenol (8) displayed a binding score of −14.043 kcal/mol with tyrosinase. In the case of 5-LOX and COX-2, the lowest binding energy was exhibited by isobetanidin (9), with an energy score of −13.168 kcal/mol and −12.740 kcal/mol, respectively. Visualization analysis revealed that the receptor's active site was occupied by all of the potential compounds. Strong interactions were displayed by all compounds, especially in the case of hyaluronidase and elastase. On the basis of the results obtained, isobetanidin was found to be a promising candidate in LPM as it shows interactions with hyaluronidase, cyclooxygenase, and lipoxygenases. The binding interactions of compounds with the lowest binding score are depicted in Fig. 3.

The process of developing a new drug involves giving significant attention to its pharmacokinetic and safety properties. In order to assess the effectiveness of the lead molecule, the ADMET properties were examined. The pharmacokinetics of the identified compounds were determined using the freely accessible web server pkCSM (Table 4). During the ADMET evaluation, the expected values of intestinal absorption serve to validate the strong therapeutic potential. Some studies have indicated that compounds with good absorption attributes have the ability to pass through the gut barrier via passive penetration in order to reach the target molecule. The estimated intestinal solubility of identified compounds confirms their good efficacy when compared to a standard value. All of the derivatives exhibited excellent intestinal solubility results in comparison to the standard value (>30 %abs). Similarly, the permeability values of the Blood Brain Barrier (BBB) was calculated for all compounds and it was compared with a standard value ranging from −1 to 0.3 log BB. Compounds with a log BB value greater than 0.3 are able to cross the BBB, while those with a value less than −1 are poorly distributed to the brain. Based on values obtained it can be postulated that all the compounds have the ability to cross BBB except touruosamine. Furthermore, the predicted metabolic actions of these compounds were found to be associated with CYP3A4, CYP2D6, and CYP2C9, which are isoforms of the cytochrome P450 enzyme. The positive results indicate that these compounds exhibit favorable metabolic behavior. Additionally, the Ames mutagenicity and hepatotoxicity of the identified compounds were assessed to determine their non-toxic potential.

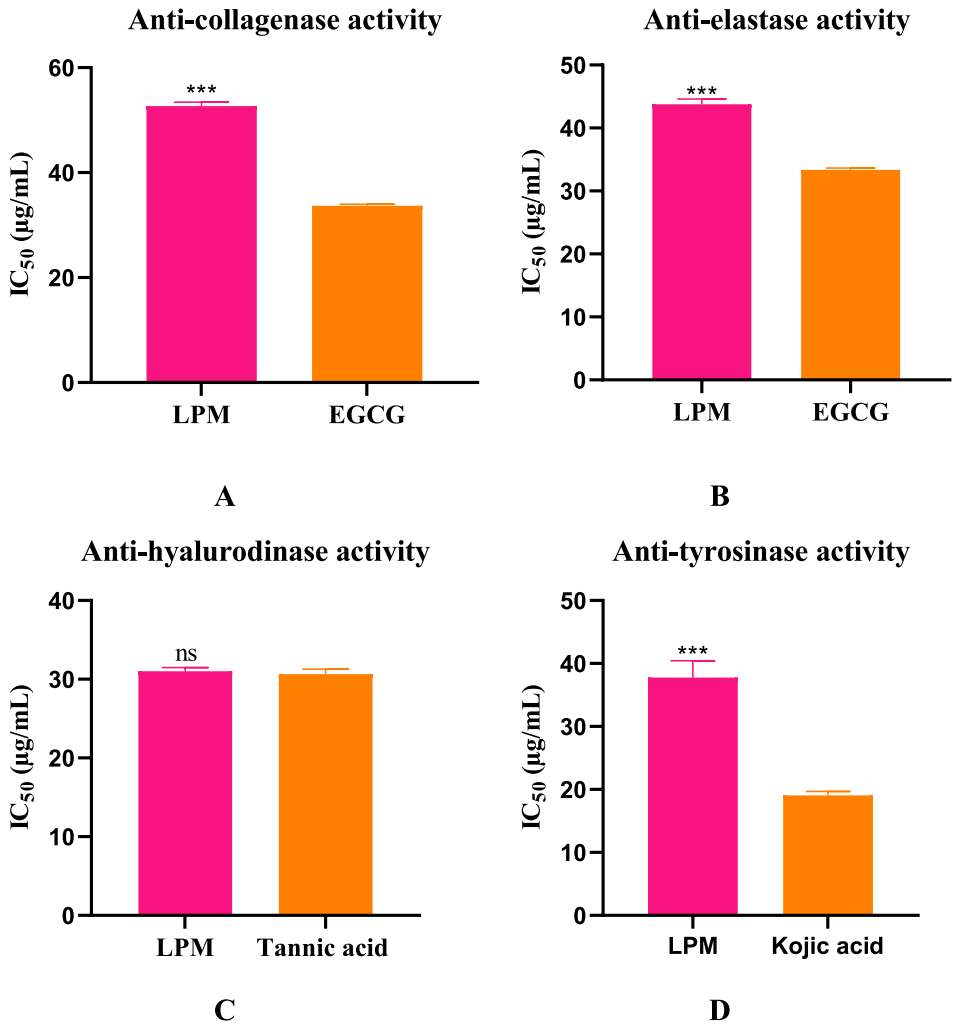

Fig. 1. Enzyme inhibitory activity of *Launaea procumbens* against (A) Collagenase, (B) elastase, (C) hyalurodinase, and (D) Tyrosinase, compared to epigallocatechin gallate (EGCG), Tannic acid, and kojic acid respectively. The data expressed as IC_{50}, a mean of three distinct and independent experiments.

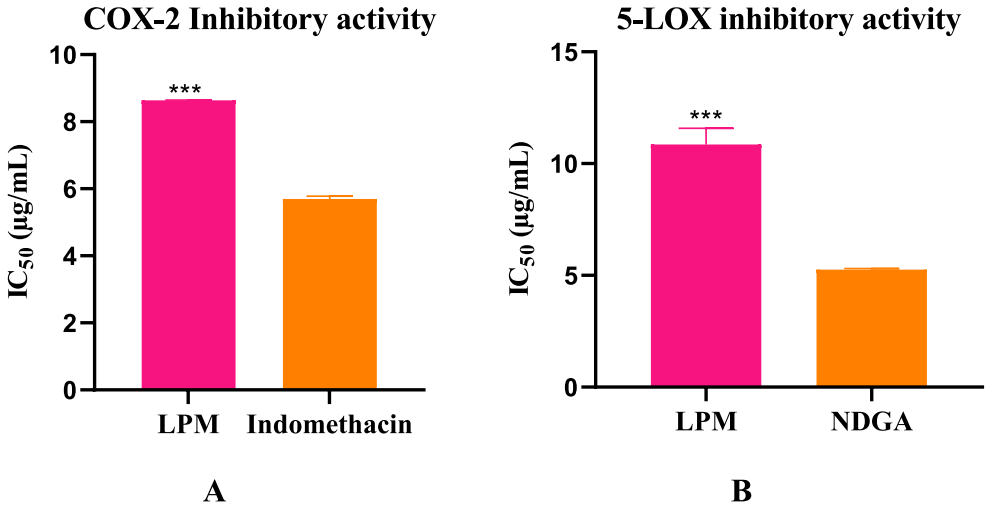

Fig. 2. Anti-inflammatory activity of *Launaea procumbens*. Inhibitory activity on (A) COX-2, and (B) 5-LOX; compared to indomethacin and Nordihydroguaiaretic acid (NDGA), respectively. The data expressed as IC_{50}, a mean of three distinct and independent experiments.

Table 2
List of Identified compounds in *Launaea procumbens* methanolic extract (LPM).

Number	Name	Chemical class
1	11(15 → 1)-Abeo-4(20),11-taxadiene-5,7,9,10,13,15-hexol; (5α,7β,9α,10β,13α)-form, 10-Benzoyl, 7,9-di-Ac	Tetracyclic diterpenoid
2	Loganic acid; 7-O-(6R-β-D-Glucopyranosyloxy-2,6-dimethyl-2E,7-octadienoyl), Me ester	Iridoid glycoside
3	Touruosamine	Alkaloid
4	Esculin	Coumarin glucoside
5	Vulgaxanthin I	Betaxanthins
6	5-caffeoylquinic acid (Chlorogenic acid)	Phenolic acid
7	3'-methoxy-4'-o-methyljoubertiaminol	Alkaloid
8	Cimigenol; 3-*O*-β-D-Galactopyranoside	Triterpenoid
9	Isobetanidin	Indolecarboxylic acid
10	Glycerol 1-alkanoates; Glycerol 1-(12-hydroxy-13E,15E-pentatriacontanoate)	Fatty acid ester
11	Bullatacinone	Lactone
12	11,12,13-Trihydroxy-9-octadecenoic acid	
13	Luteolin 8-C-glucoside	Flavonoid glycoside
14	Phytol	acyclic diterpene alcohol
15	Fumaflorine; Me ester	Alkaloid
16	Catechin-5-*O*-glucoside	Phenolic compound

4. Discussion

The aging process is an unavoidable and natural process that impacts multiple body parts, with the skin being one of the most visible parts that experiences significant alterations over time (Ndlovu et al., 2013). The perception and impact of skin aging can vary among individuals and across different cultures. The societal emphasis on youthful appearance can contribute to psychological impacts, affecting self-esteem and well-being worldwide. Various skin anti-aging products and treatments are available to address the signs of aging and promote younger-looking skin (Gupta and Gilchrest, 2005). The use of botanicals and their constituents as cosmeceuticals has gained popularity in recent years. This has led to the development of the aging-related cosmeceuticals market, which is currently one of the largest consumer markets (Younis et al., 2022). One of the major contributors to skin aging is UV radiation. Exposure to UV radiation triggers the generation of reactive oxygen species (ROS), leading to oxidative stress, the breakdown of collagen and elastin in the ECM, and inflammation. Therefore, antioxidant supplements protect the skin from environmental pollutants and are designed to combat oxidative stress and premature aging (Huang et al., 2013). LPM extract demonstrated considerable antioxidant activity in both DPPH and FRAP assays. The anti-oxidant capacity of LPM could be attributed to their phenolic content, which plays a crucial role in quenching ROS. The phytochemical profile of LPM extract (Table 3) revealed that the extract contains flavonoids, phenolic compounds, and coumarin. Flavonoids and phenolic compounds are powerful antioxidants that protect the skin against UV radiation, oxidative stress, and related inflammation, so they protect the skin from aging by different mechanisms (Zofia et al., 2020). The formerly described antioxidant activities of 5-caffeoylquinic acid (Segheto et al., 2018, Chen et al., 2020, Boulebd et al., 2023), luteolin 8-C-glucoside (Choi et al., 2014, Zielińska and Zieliński, 2011), and catechin-5-O-glucoside (Rao et al., 2018, Rao et al., 2020) verify their contribution to the antioxidant potential of LPM extract.

Collagen and elastin are crucial proteins in the ECM structure responsible for skin strength and flexibility. Collagen network and elastin fiber degradation with aging causes the appearance of wrinkles and fine lines as visible signs of aging. These two proteins are degraded during aging due to the overactivation of collagenase and elastase enzymes, respectively. Another key component of the ECM is hyaluronic acid, which keeps the skin moist, well hydrated, and smooth. Hyaluronidase enzyme controls the degradation of hyaluronic acid. Additionally, tyrosine is a precursor for the synthesis of melanin, the pigment responsible for the color of the skin, hair, and eyes. Tyrosinase is the rate-limiting enzyme in melanin production. While tyrosinase is not directly implicated in the structural aging of the skin, overproduction of melanin, which causes changes in pigmentation (such as age spots or hyperpigmentation), can be associated with the aging process (Cruz et al., 2023). Extrinsic factors such as UV radiation can increase the activity of collagenase, elastase, hyaluronidase, and tyrosinase enzymes, causing the degradation of the ECM and the formation of photoaging signs (Elgamal et al., 2021, Fikry et al., 2023). Hence, strategies to inhibit these enzymes are a useful strategy in fighting against aging and delaying aging signs and hyperpigmentation. Enzyme inhibitors may have therapeutic potential in the fields of dermatology and cosmetic medicine (Cruz et al., 2023). In this study, LPM extract was evaluated to inhibit aging enzymes by *in vitro* enzyme inhibition assays. The extract showed promising enzyme-inhibition activity against the four enzymes. The strongest activity was anti-hyaluronidase, followed by collagenase and elastase inhibition activity, while the least activity was against the tyrosinase enzyme. Compounds previously characterized in LPM extract were reported to exhibit enzyme inhibition activity. For example, catechecin has been shown to exhibit moderate collagenase and elastase inhibitory activity (Wittenauer et al., 2015). As well, luteolin derivatives were found to have inhibitory activity on collagenase, elastase, and hyaluronidase enzymes and reversible noncompetitive inhibition of the tyrosinase enzyme (Acıkara et al., 2019, Wijaya et al., 2020, Zhang et al., 2017). Similar results were obtained from the investigation of *Hypericum calycinum,* which contains an abundant amount of chlorogenic acid and exhibited promising *in vitro* anti-aging potential by interfering with these enzymes (Ersoy et al., 2019). Phytol diterpene identified in LPM was used in cosmetics to inhibit cellular senescence of keratinocytes caused by oxidative stress. It also exhibited antioxidant and anti-inflammatory activity (Younis et al., 2022). Previous molecular docking studies revealed that phytol can bind to the amino acid residues in collagenase enzyme catalytic domain with binding energy comparable to that of the reference compound doxycycline (Yasmeen and Gupta, 2019).

In this work, we also aimed to investigate the anti-inflammatory activity of LPM with the goal of having integral insights about the possibility of developing a new natural skin anti-aging cosemeceutical. Skin aging is closely related to inflammation, which is characterized by elevated levels of pro-inflammatory mediators. Lipoxygenase (LOX) enzymes induce the release of pro-inflammatory mediators like leukotrienes. Increased LOX activity can result in the excessive production of such mediators. Pro-inflammatory mediators accelerate the aging process, causing the appearance of wrinkles, decreased tissue repair, and loss of elasticity. Cyclooxygenase (COX) enzymes convert archidonic acid into prostaglandins. Overproduction of COX enzymes can result in excessive prostaglandin synthesis, producing persistent tissue inflammation and hastening the aging process. Also, excessive prostaglandins can contribute to the breakdown of collagen and elastin, resulting in wrinkles and a loss of skin elasticity (Younis et al., 2023, Fuller, 2019, Guimarães et al., 2021). So the assessment of anti-inflammatory activity was performed to determine the indirect effects of aging on skin characteristics. LPM extract exhibited a promising and comparable inhibitory activity to that of indomethacin on COX-2. Furthermore, LPM exhibited potent 5-LOX inhibitory activity. Among the identified compounds, loganic acid iridoid showed pronounced anti-inflammatory effects by decreasing TNF-α and IL-6 activity (Sozański et al., 2016, Wei et al., 2013). In the same context, esculin was reported to have potent anti-inflammatory activities in vivo and *in vitro* via inhibition of the MAPK pathway (Niu et al., 2015), and likewise, esculin inhibited inflammatory cells and proinflammatory cytokines including TNF-α, IL-1β, and IL-6 in LPS-induced acute lung injury (Tianzhu and Shumin, 2015). In addition, several studies documented the anti-inflammatory activity of chlorogenic (Hwang et al., 2014, Shin et al., 2015), luteolin (Aziz et al., 2018) and catechin (Sunil et al., 2021). Molecular docking has been utilized as a useful approach for anticipating the likely interaction

Table 3
Binding interactions between anti-aging enzymes (collagenase, elastase, hyaluronidase and tyrosinase) with identified compounds of *Launaea procumbens* methanolic extract (LPM).

Compound (NO.)	Hyaluronidase		Elastase		Tyrosinase		Collagenase	
	Score (Kcal/mol)	Amino acid Residue/Bond	Score (Kcal/mol)	Amino acid Residue/Bond	Score (Kcal/mol)	Amino acid Residue/Bond	Score (Kcal/mol)	Amino acid Residue/Bond
11(15 → 1)-Abeo-4(20),11-taxadiene-5,7,9,10,13,15-hexol; (5α,7β,9α,10β,13α)-form, 10-Benzoyl, 7,9-di-Ac **(1)**	−10.187	Gln259/H-donor Lys377/H-donor Glu415/H-donor Glan259/H-acceptor	−10.632	Thr41/H-donor Arg143/H-acceptor	−10.387	Asp336/H-donor	−9.468	Tyr237/H-donor
Loganic acid; 7-O-(6R-β-D-Glucopyranosyloxy-2,6-dimethyl-2E,7-octadienoyl), Me ester **(2)**	−13.559	Leu381/H-donor Asp408/H-donor Glu415/H-donor Gln411/H-acceptor Met412/H-acceptor	−14.497	Thr41/H-donor Arg143/H-acceptor	−12.729	Asp336/H-donor	−11.877	Asn180/H-donor Glu219/H-donor Leu181/H-acceptor
Touruosamine **(3)**	−11.566	Asn383/H-acceptor	−10.904	Tyr35/H-donor Thr41/H-acceptor	−10.011	Glu335/H-donor	−13.953	Tyr237/H-acceptor
Esculin **(4)**	−12.423	Glu407/H-donor Asp408/H-donor Asn383/H-acceptor	−14.819	Tyr35/H-donor Thr41/H-acceptor Arg63/H-acceptor	−11.080	Glu317/H-donor Asp336/H-donor	−13.712	Tyr237/H-donor Ser239/H-donor
Vulgaxanthin I **(5)**	−12.729	Gln259/H-donor Lys377/H-donor	−13.661	Ser151/H-donor Arg39/H-acceptor Arg63/H-acceptor	−10.517	Asp336/H-donor	−13.812	Hie228/H-donor Thr103/H-acceptor
Chlorogenic acid **(6)**	−14.117	Leu379/H-donor Glu415/H-donor	−15.163	Thr41/H-donor Ser151/H-donor Arg63/H-acceptor	−11.502	Glu317/H-donor Asp336/H-donor Asp353/H-donor	−13.883	Hie228/H-donor
3'-methoxy-4'-o-methyljoubertiaminol **(7)**	−11.847	Leu379/H-donor Glu415/H-donor	−10.329	Tyr35/H-donor Thr41/H-donor Ser36/H-acceptor	−10.614	Glu335/H-donor	−9.825	Asn180/H-donor Glu219/H-donor Leu181/H-acceptor
Cimigenol; 3-O-β-D-Galactopyranoside **(8)**	−11.637	Leu379/H-donor Glu415/H-donor	−12.989	Tr9141/H-donor Ser151/H-donor Arg39/H-acceptor Arg63/H-acceptor	−14.043	Glu335/H-donor Asp353/H-donor	−12.633	Tyr237/H-acceptor
Isobetanidin **(9)**	−15.154	Glu407/H-donor Asp408/H-donor	−14.458	Thr41/H-donor Arg39/H-acceptor Arg143/H-acceptor	−12.047	Glu335/H-donor	−13.359	Hie228/H-donor
Glycerol-1-alkanoates:glycerol-1-(12-hydroxy-13E, 15E-pentatria-contanoate **(10)**	−11.661	Lys377/H-donor Asp408/H-donor	−9.532	Tyr35/H-donor Trp141/H-donor Ser151/H-donor	−11.249	Glu335/H-donor	−10.688	Asp186/H-donor
Bullatacinone **(11)**	−10.503	Glu415/H-donor Leu381/H-acceptor	−11.392	Trp151/H-donor Ser151/H-donor Arg143/H-acceptor	−10.071	Glu335/H-donor Thr360/H-acceptor	−11.081	Tyr237/H-donor
11,12,13-Trihydroxy-9-octadecenoic acid **(12)**	−13.750	Glu304/H-donor Glu415/H-donor	−13.143	Cys58/H-donor Tyr65/H-donor Arg39/H-acceptor	−9.908	Asp353/H-donor	−11.543	Thr230/H-donor
Luteolin 8-C-glucoside **(13)**	−14.805	Asp408/H-donor Asn383/H-acceptor	−16.814	Thr41/H-donor Tyr35/H-acceptor Arg63/H-acceptor	−7.340		−13.560	Thr103/H-donor Asp186/H-donor Ser227/H-donor
Phytol **(14)**	−10.466	Ser405/H-donor Glu407/H-donor	−10.063	Thr41/H-donor Cys58/H-donor Arg63/H-acceptor	−9.567	Asp353/H-donor	−10.047	Tyr237/H-donor
Fumaflorine; Me ester **(15)**	−12.172	Asn383/H-acceptor	−12.307	Ser151/H-acceptor	−9.995		−11.677	Tyr237/H-acceptor
Catechin-5-O-glucoside **(16)**	−14.936	Glu304/H-donor Leu379/H-acceptor	−14.116	Hie40/H-donor Thr41/H-donor Cys58/H-donor	−13.168	Val325/H-donor Glu317/H-donor	−12.447	Asp186/H-donor

of new pharmacological drugs with target proteins, therefore aiding in the prediction of potential mechanisms of action (Ahmed et al., 2022). Molecular docking was employed in the present work to examine the mechanisms of action of previously characterized compounds in LPM extract. In order to choose the best ligand interaction, each ligand is docked independently with the selected enzymes. The scores and poses that are produced are then compared, with the assumption that the lowest score indicates the best binding affinity. Compounds interacting with active site residues demonstrated their ability to inhibit the selected enzymes. Isobetanidin was found to be a promising antiaging candidate in the plant as it shows interactions with hyaluronidase, cyclooxygenase, and lipoxygenases. The results are consistent with a previous study that proved the inhibitory activity of betalain-enriched beetroots containing isobetandin on both hyaluronidase and

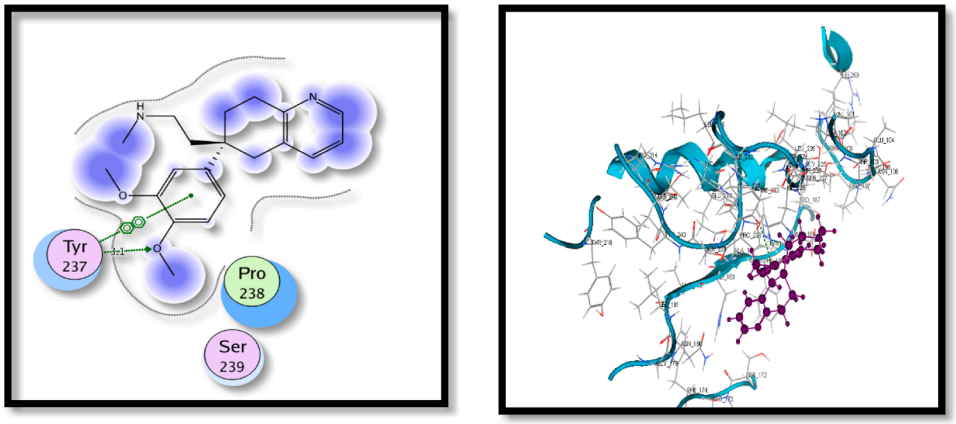

A

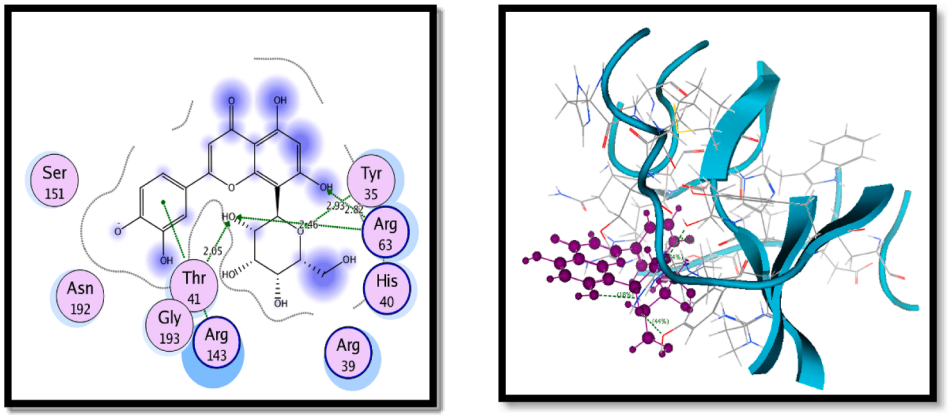

B

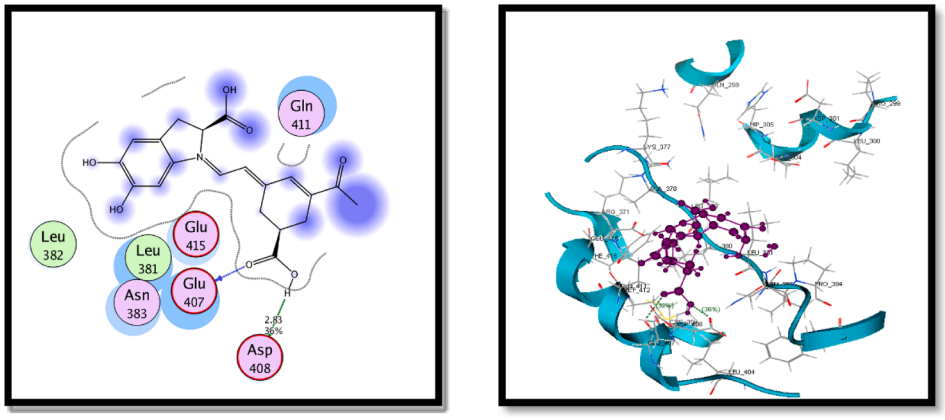

C

Fig. 3. 2D and 3D binding mode representation of top most compounds in binding pocket of selected targets. (A) Touruosamine-collagenase complex, (B) Luteolin 8-C-glucoside- Elastase complex ((C) Isobetanidin-hyaluronidase complex, (D), Cimigenol-tyrosinase complex, (E) Isobetanidin-5-LOX complex, (F) Isobetanidin-COX complex.

lipoxygenase enzymes (Saad et al., 2023). Therefore, the observed significant antioxidant, anti-aging, and anti-inflammatory activities of LPM extract are attributed to the synergistic effects of all its constituents. We believe that our results pave the way for the incorporation of LPM extract in anti-aging products. Further in vivo biological studies using topical formulations containing LPM extract are planned and

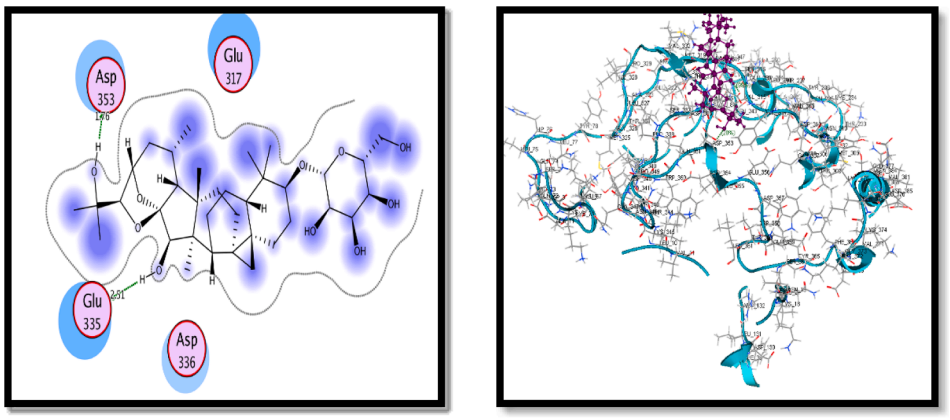

D

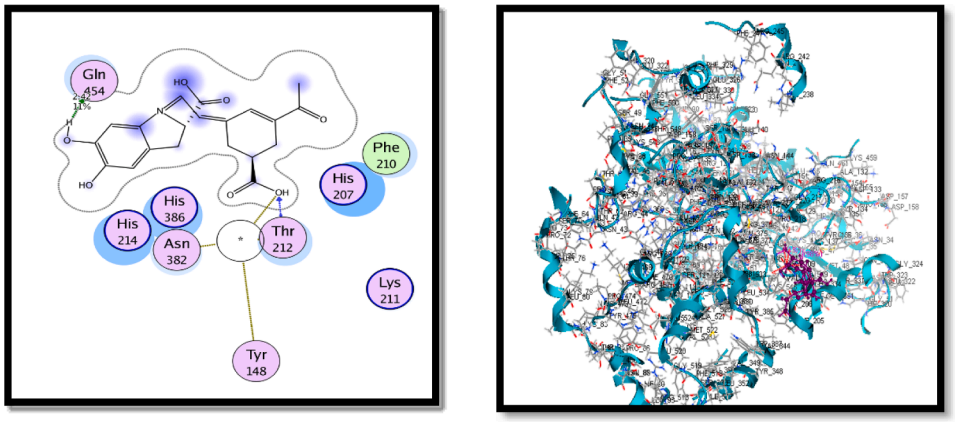

E

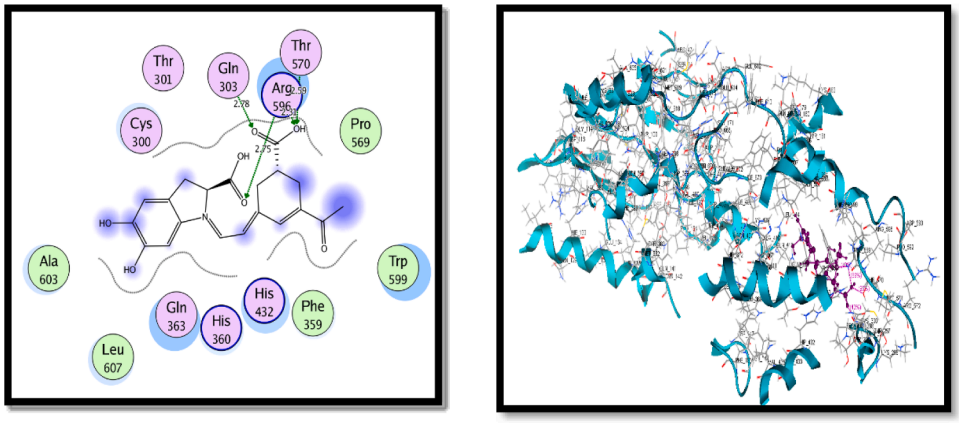

F

Fig. 3. (*continued*).

highlighted as future work to validate the *in vitro* results.

5. Conclusion

The use of botanicals and their constituents as cosmeceuticals has gained popularity in recent years. Our study revealed the appreciable antioxidant activity of *Launaea procumbens* extract. The extract as well showed considerable inhibitory activity for collagenase, elastase, hyalurondinase, and tyrosinase enzymes, which play a significant role in aging skin. Natural inhibitors of the aforementioned enzymes represent evolving and promising candidates that could be used as a safe alternative for skin aging, particularly if these inhibitors possess antioxidant

Table 4
ADMET results of identified compounds of *Launaea procumbens* methanolic extract (LPM).

Compound	Intestinal absorption	BBB	CYP3A4 substrate	CYP2C9 substrate	CYP2D6 substrate	CYP3A4 Inhibitor	CYP2C9 Inhibitor	CYP2D6 Inhibitor	AMES mutagenesis	Acute oral toxicity (LD50)	Hepato-toxicity
11(15 → 1)-Abeo-4(20),11-taxadiene-5,7,9,10,13,15-hexol; (5α,7β,9α,10β,13α)-form, 10-Benzoyl, 7,9-di-Ac	84.36	−1.118	Yes	No	No	No	No	No	No	2.69	No
Loganic acid; 7-O-(6R-β-D-Glucopyranosyloxy-2,6-dimethyl-2E,7-octadienoyl), Me ester	0	−2.379	No	No	No	No	No	No	No	2.97	No
Touruosamine	98.29	−0.019	Yes	No	No	No	No	Yes	No	2.83	yes
Esculin	52.65	−1.476	No	No	No	No	No	No	No	2.693	Yes
Vulgaxanthin I	0	−1.441	No	No	No	No	No	No	No	2.371	Yes
Chlorogenic acid	8.851	−1.785	No	No	No	No	No	No	No	2.631	No
3'-methoxy-4'-o-methyljoubertiaminol	84.36	−1.118	Yes	No	No	No	No	No	No	2.691	No
Cimigenol; 3-O-β-D-Galactopyranoside	48.17	−1.165	Yes	No	No	No	No	No	No	4.133	No
Isobetanidin											
Glycerol-1-alkanoates: glycerol-1-(12-hydroxy-13E, 15E-pentatriacontanoate	83.03	−1.645	Yes	No	No	No	No	No	No	4.206	No
Bullatacinone	90.51	−0.723	Yes	No	No	No	No	No	No	3.915	No
11,12,13-Trihydroxy-9-octadecenoic acid	38.78	−1.427	No	No	No	No	No	No	No	2.691	No
Luteolin 8-C-glucoside	45.32	−1.982	No	No	No	No	No	No	Yes	3.055	No
Phytol	90.32	0.793	Yes	No	No	No	No	No	No	1.705	No
Fumaflorine; Me ester	100	−1.206	Yes	No	No	Yes	No	No	No	3.148	Yes
Catechin-5-O-glucoside	31.82	−1.939	No	No	No	No	No	No	Yes	2.768	No

activity. Furthermore, the plant extract exhibited significant inhibition of cycloxgenase (COX-2) and lipoxygenase-5 (LOX-5) enzymes, which are key enzymes in the development of inflammation. The observed significant antioxidant, anti-aging, and anti-inflammatory activities of LPM extract are attributed to the synergistic effects of all its constituents. The identified compounds showed a high potential to bind to the active sites of target enzymes. ADMET analysis of the compounds revealed their good absorption, distribution, and metabolism profiles, and they were found to be safe as well. These findings assist in the incorporation of *Launaea procumbens* extract in cosmetics for fighting and delaying skin aging after further investigations. We believe that our results pave the way for the incorporation of LPM extract in anti-aging products. Further in vivo biological studies using topical formulations containing LPM extract are planned and highlighted as future work to validate the *in vitro* results.

Funding

This research did not receive any specific grant from funding agencies.

CRediT authorship contribution statement

Hanan Khojah: Conceptualization, Writing – review & editing. **Shaima R. Ahmed:** Conceptualization, Writing – review & editing. **Shahad Y. Alharbi:** Investigation, Writing – original draft. **Kholood K. AlSabeelah:** Investigation, Software, Writing – original draft. **Hatham Y. Alrayyes:** Investigation, Software, Writing – original draft. **Kadi B. Almusayyab:** Investigation, Software, Writing – original draft. **Shahad R. Alrawiliy:** Investigation, Writing – original draft. **Raghad M. Alshammari:** Investigation, Writing – original draft. **Sumera Qasim:** Software, Validation.

Declaration of competing interest

The authors declare that they have no known competing financial interests or personal relationships that could have appeared to influence the work reported in this paper.

References

Acıkara, Ö.B., Ilhan, M., Kurtul, E., Šmejkal, K., Akkol, E.K., 2019. Inhibitory activity of *Podospermum canum* and its active components on collagenase, elastase and hyaluronidase enzymes. Bioorg. Chem. 93, 103330.

Ahmed, S.R., Mostafa, E.M., Musa, A., Rateb, E.E., Al-Sanea, M.M., Abu-Baih, D.H., Elrehany, M.A., Saber, E.A., Rateb, M.E., Abdelmohsen, U.R., 2022. Wound Healing and Antioxidant Properties of *Launaea procumbens* Supported by Metabolomic Profiling and Molecular Docking. Antioxidants. 11, 2258.

Aziz, N., Kim, M.-Y., Cho, J.Y., 2018. Anti-inflammatory effects of luteolin: A review of in vitro, in vivo, and in silico studies. J. Ethnopharmacol. 225, 342–358.

Boulebd, H., Carmena-Bargueño, M., Pérez-Sánchez, H., 2023. Exploring the antioxidant properties of caffeoylquinic and feruloylquinic acids: a computational study on hydroperoxyl radical scavenging and xanthine oxidase inhibition. Antioxidants. 12, 1669.

Chen, X., Yang, J.H., Cho, S.S., Kim, J.H., Xu, J., Seo, K., Ki, S.H., 2020. 5-Caffeoylquinic acid ameliorates oxidative stress-mediated cell death via Nrf2 activation in hepatocytes. Pharm. Biol. 58, 999–1005.

Choi, J.S., Islam, M.N., Ali, M.Y., Kim, Y.M., Park, H.J., Sohn, H.S., Jung, H.A., 2014. The effects of C-glycosylation of luteolin on its antioxidant, anti-Alzheimer's disease, anti-diabetic, and anti-inflammatory activities. Arch. Pharmacal Res. 37, 1354–1363.

Cruz et al., 2023, R., Liakou, A. I., Theodoridis, A., Makrantonaki, E., Zouboulis, C. C., Skin anti-aging strategies. Derm.-Endocrinol. 4, 308-319.

Cruz, A.M., Gonçalves, M.C., Marques, M.S., Veiga, F., Paiva-Santos, A.C., Pires, P.C., 2023a. In vitro models for anti-aging efficacy assessment: a critical update in dermocosmetic research. Cosmetics. 10, 66.

Elgamal, A.M., El Raey, M.A., Gaara, A., Abdelfattah, M.A., Sobeh, M., 2021. Phytochemical profiling and anti-aging activities of *Euphorbia retusa* extract: in silico and in vitro studies. Arabian J. Chem. 14, 103159.

Ersoy, E., Ozkan, E.E., Boga, M., Yilmaz, M.A., Mat, A., 2019. Anti-aging potential and anti-tyrosinase activity of three *Hypericum* species with focus on phytochemical composition by LC–MS/MS. Ind. Crops Prod. 141, 111735.

Fikry, E., Mahdi, I., Ortaakarsu, A.B., Tawfeek, N., Ochieng, M.A., Bakrim, W.B., Abdelfattah, M.A., Omari, K.W., Mahmoud, M.F., Sobeh, M., 2023. Dermato-

cosmeceutical properties of *Pseudobombax ellipticum* (Kunth) Dugand: Chemical profiling, in vitro and in silico studies. Saudi Pharm. J. 31, 101778.
Fuller, B., 2019. Role of PGE-2 and other inflammatory mediators in skin aging and their inhibition by topical natural anti-inflammatories. Cosmetics. 6, 6.
Gilaberte, Y., Prieto-Torres, L., Pastushenko, I., Juarranz, Á., 2016. Anatomy and Function of the Skin. Nanosci. Dermatol. 1–14.
Guimarães, G.R., Almeida, P.P., de Oliveira Santos, L., Rodrigues, L.P., de Carvalho, J.L., Boroni, M., 2021. Hallmarks of aging in macrophages: Consequences to skin inflammaging. Cells. 10, 1323.
Gupta, M.A., Gilchrest, B.A., 2005. Psychosocial aspects of aging skin. Dermatol. Clin. 23, 643–648.
Huang, B., Zhu, L., Liu, S., Li, D., Chen, Y., Ma, B., Wang, Y., 2013. In vitro and in vivo evaluation of inhibition activity of lotus (*Nelumbo nucifera* Gaertn.) leaves against ultraviolet B-induced phototoxicity. J. Photochem. and Photobiolo. b: Biol. 121, 1–5.
Hwang, S.J., Kim, Y.-W., Park, Y., Lee, H.-J., Kim, K.-W., 2014. Anti-inflammatory effects of chlorogenic acid in lipopolysaccharide-stimulated RAW 264.7 cells. Inflammation Res. 63, 81–90.
Khan, R.A., Khan, M.R., Sahreen, S., 2010. Evaluation of *Launaea procumbens* use in renal disorders: A rat model. J. Ethnopharmacol. 128, 452–461.
Khan, R.A., Khan, M.R., Sahreen, S., Ahmed, M., 2012. Assessment of flavonoids contents and in vitro antioxidant activity of *Launaea procumbens*. Chem. Cent. J. 6, 1–11.
Lawton, S., 2019. Skin 1: the structure and functions of the skin. Nurs. times. 115, 30–33.
Makasana, A., Ranpariya, V., Desai, D., Mendpara, J., Parekh, V., 2014. Evaluation for the anti-urolithiatic activity of *Launaea procumbens* against ethylene glycol-induced renal calculi in rats. Toxicol. Rep. 1, 46–52.
Ndlovu, G., Fouche, G., Tselanyane, M., Cordier, W., Steenkamp, V., 2013. In vitro determination of the anti-aging potential of four southern African medicinal plants. BMC Complementary Altern. Med. 13, 1–7.
Niu, X., Wang, Y., Li, W., Zhang, H., Wang, X., Mu, Q., He, Z., Yao, H., 2015. Esculin exhibited anti-inflammatory activities in vivo and regulated TNF-α and IL-6 production in LPS-stimulated mouse peritoneal macrophages in vitro through MAPK pathway. Title Int. Immunopharmacol. 29, 779–786.
Parekh, J., Chanda, S., 2006. In-vitro antimicrobial activities of extracts of *Launaea procumbens* roxb. (Labiateae), *Vitis vinifera* l. (Vitaceae) and *Cyperus rotundus* l. (Cyperaceae). Afr. J. of Biomed. Res. 9.
Rao, S., Santhakumar, A.B., Chinkwo, K.A., Blanchard, C.L., 2018. Q-TOF LC/MS identification and UHPLC-Online ABTS antioxidant activity guided mapping of barley polyphenols. Food Chem. 266, 323–328.
Rao, S., Santhakumar, A.B., Chinkwo, K.A., Blanchard, C.L., 2020. Investigation of phenolic compounds with antioxidant activity in barley and oats affected by variation in growing location. Cereal Chem. 97, 772–782.
Rawat, P., Saroj, L.M., Kumar, A., Singh, T.D., Tewari, S., Pal, M., 2016. Phytochemicals and cytotoxicity of *Launaea procumbens* on human cancer cell lines. Pharmacogn. Mag. 12, S431.
Reddy, M., Mishra, G.J., 2012. Preliminary phytochemical screening and antibacterial analysis of the leaf extracts of *Launaea procumbens* Roxb. Int. J. Phytopharm. 3, 147–151.
Saad, F., Al-Shaikh, T.M., Zouidi, F., Taher, M.A., Saidi, S.A., Hamden, K. 2023. Betalain-Enriched Beetroots Exhibit Antiulcer and Anti-inflammatory Potentials. J. Food Process. Preserv. 2023.
Segheto, L., Santos, B.C.S., Werneck, A.F.L., Vilela, F.M.P., de Sousa, O.V., Rodarte, M.P., 2018. Antioxidant extracts of coffee leaves and its active ingredient 5-caffeoylquinic acid reduce chemically-induced inflammation in mice. Ind. Crops Prod. 126, 48–57.
Shin, H.S., Satsu, H., Bae, M.-J., Zhao, Z., Ogiwara, H., Totsuka, M., Shimizu, M., 2015. Anti-inflammatory effect of chlorogenic acid on the IL-8 production in Caco-2 cells and the dextran sulphate sodium-induced colitis symptoms in C57BL/6 mice. Food Chem. 168, 167–175.
Sozański, T., Kucharska, A.Z., Rapak, A., Szumny, D., Trocha, M., Merwid-Ląd, A., Dzimira, S., Piasecki, T., Piórecki, N., Magdalan, J., 2016. Iridoid–loganic acid versus anthocyanins from the Cornus mas fruits (cornelian cherry): Common and different effects on diet-induced atherosclerosis, PPARs expression and inflammation. Atherosclerosis. 254, 151–160.
Sunil, M., Sunitha, V., Santhakumaran, P., Mohan, M.C., Jose, M.S., Radhakrishnan, E., Mathew, J., 2021. Protective effect of (+)–catechin against lipopolysaccharide-induced inflammatory response in RAW 264.7 cells through downregulation of NF-κB and p38 MAPK. Inflammopharmacology. 29, 1139–1155.
Tianzhu, Z., Shumin, W., 2015. Esculin inhibits the inflammation of LPS-induced acute lung injury in mice via regulation of TLR/NF-κB pathways. Inflammation. 38, 1529–1536.
Wazi, S.M., Saima, S., Dasti, A.A., Subhan, S., 2007. Ethanobotnical importance of Salt range species of District Karak. Pakistan. Pak. J. Plant Sci. 13, 29–31.
Wei, S., Chi, H., Kodama, H., Chen, G., 2013. Anti-inflammatory effect of three iridoids in human neutrophils. Nat. Prod. Res. 27, 911–915.
Wei, K., Louis, H., Emori, W., Idante, P.S., Agwamba, E.C., Cheng, C.R., Unimuke, T.O., 2022. Antispasmodic activity of carnosic acid extracted from rosmarinus officinalis: Isolation, spectroscopic characterization, DFT studies, and in silico molecular docking investigations. J Mol. Str. 1260, 132795.
Wijaya, L., Lister, I.N.E., Fachrial, E., Girsang, E., 2020. Scavenge ABTS and Inhibition of Elastase Enzyme Activity from Ethanol Extract of Pineapple (Annas cosmusus (L.) Merr) Core. ASRJETS. 70, 106–113.
Wittenauer, J., Mäckle, S., Sußmann, D., Schweiggert-Weisz, U., Carle, R., 2015. Inhibitory effects of polyphenols from grape pomace extract on collagenase and elastase activity. Fitoterapia. 101, 179–187.
Yasmeen, S., Gupta, P., 2019. Interaction of selected terpenoids from Dalbergia sissoo with catalytic domain of matrix metalloproteinase-1: An in silico assessment of their anti-wrinkling potential. Bioinf. Biol. Insights. 13, 1177932219896538.
Younis, M.M., Ayoub, I.M., Mostafa, N.M., El Hassab, M.A., Eldehna, W.M., Al-Rashood, S.T., Eldahshan, O.A., 2022. GC/MS profiling, anti-collagenase, anti-elastase, anti-tyrosinase and anti-hyaluronidase activities of a *Stenocarpus sinuatus* leaves extract. Plants. 11, 918.
Younis, I.Y., Farag, M.A., Elgamal, A.M., Mohsen, E., 2023. Untargeted metabolites profiling of volatile and non-volatile components of Egyptian lotus (*Nelumbo nucifera* Gaertn.) using UHPLC/PDA/ESI-MS and solid-phase microextraction (SPME) GC/MS in relation to its antiaging and anti-inflammatory effects. Ind. Crops Prod. 197, 116561.
Zhang, L., Zhao, X., Tao, G.-J., Chen, J., Zheng, Z.-P., 2017. Investigating the inhibitory activity and mechanism differences between norartocarpetin and luteolin for tyrosinase: A combinatory kinetic study and computational simulation analysis. Food Chem. 223, 40–48.
Zielińska, D., Zieliński, H., 2011. Antioxidant activity of flavone C-glucosides determined by updated analytical strategies. Food Chem. 124, 672–678.
Zofia, N.-Ł., Martyna, Z.-D., Aleksandra, Z. , Tomasz, B., 2020. Comparison of the antiaging and protective properties of plants from the Apiaceae family. Oxid. Med. Cell. Longevity. 2020.